Technical University of Denmark

DTU

Identifying isomers of C-78 by means of x-ray spectroscopy

Bassan, Arianna; Nyberg, Mats; Luo, Yi

DTU Library
Technical Information Center of Denmark

Identifying isomers of C$_{78}$ by means of x-ray spectroscopy

Arianna Bassan

Department of Physics, University of Stockholm, SCFAB, S-106 91 Stockholm, Sweden

Mats Nyberg

Department of Physics, Technical University of Denmark, DK-2800 Lyngby, Denmark

Yi Luo*

Theoretical Chemistry, Royal Institute of Technology, SCFAB, S-10691 Stockholm, Sweden

X-ray photoelectron and absorption spectra of C$_{78}$ isomers have been generated using density functional theory with inclusion of the full core-hole potentials. Strong isomer dependence has been found in absorption, but not in the photoelectron spectra. C$_{78}$ isomers can be thought to be formed by inserting 18 carbon atoms into an opened C$_{60}$. We have shown how the different local arrangements of these 18 carbon atoms are responsible for the significant isomer dependence observed. Our calculated spectra are in excellent agreement with the experimental counterparts.

I. INTRODUCTION

The discovery of fullerenes[1] ushered in an era of fascinating studies, both theoretical and experimental, on the pleasing geodesic structures and the interesting chemical and physical properties of this new class of molecules. Straightforward preparation of macroscopic amounts of the two smallest members of the fullerene family, namely, C$_{60}$ and C$_{70}$, has favored abundant investigations, which, in turn, have led to a relatively thorough picture of the properties of C$_{60}$ and C$_{70}$. On the other hand, the difficulties encountered in the production and purification of the higher members of the fullerene family have strongly limited a comprehensive insight of the properties of larger fullerenes. Moreover, these large fullerenes can exist in different isomeric forms, whose rather difficult separation has contributed to shackle extensive investigations on their properties. So far, mostly ^{13}C nuclear magnetic resonance studies have been employed in order to characterize the various isomers of higher fullerenes,[2–7] and to a smaller extent infrared, Raman, and electronic spectroscopies.[8,9]

In the specific case of C$_{78}$, five different isomers are predicted to exist by the isolated-pentagon rule.[10] Two of these five isomers have D_{3h} symmetry and have never been observed experimentally. The other three have been isolated and characterized;[3–5] one has D_3 symmetry and the remaining two interestingly belong to the same point group C_{2v} differing only in the number of no equivalent atoms and overall geometric appearance. Studies on the electronic structure of these two C_{2v} isomers have recently been performed through the use of electron-energy loss spectroscopy and ultraviolet photoemission spectroscopy.[11] Different features are present in the two C1s excitation spectra for the C_{2v} isomers and in principle these spectroscopical properties can be employed as a tool to distinguish and characterize the different isomeric forms of higher fullerenes.

In the present paper, we explore the carbon K-shell ($1s$) excitation spectra for the D_3 and C_{2v} isomers of C$_{78}$ by means of quantum chemical calculations and we discuss the sensitivity of x-ray absorption (XA) spectra to the different isomeric forms. Isomer sensitivity of ionization potentials, corresponding to the x-ray photoelectron spectroscopy (XPS), is also considered.

Spectra are computed using density functional theory (DFT), allowing inclusion of exchange and correlation effects at a reasonable computational cost that has proved to be a powerful method for the study of XA spectra (XAS).[12–15] Previous investigations on C$_{60}$ and C$_{70}$ (Ref. 14) showed that the method provides accurate oscillator strengths for those cases where valence orbitals are highly delocalized and for which excitonic effects can be present, e.g., fullerenes.

II. THEORETICAL DETAILS

The fullerenes considered in this work were fully geometry optimized using *density functional theory* at the B3LYP/6-31G level using the GAUSSIAN 98 suite of programs.[16] The obtained geometries are then used for generation of XAS and *x-ray photoelectron* spectra. For this purpose we used the program DEMON[17] that implements the Kohn-Sham approach to DFT at the gradient corrected generalized gradient approximation (GGA) level, in this case with the exchange functional by Perdew and Wang[18] combined with the correlation functional by Perdew.[19] The choice of this exchange-correlation potential has previously proven to provide excellent oscillator strengths in comparison to experiments.[14] The computational approach used in this paper follows the *static exchange* approximation[20] within a full core-hole potential representing the excited states. For this full core-hole potential we first generate the total density in a good molecular basis set, and then diagonalize the Kohn-Sham matrix in a much larger basis set consisting of additional (19s, 19p, 19d) diffuse functional basis, which is added onto the molecular basis set where the core-hole is located (corresponding to the atom where the excitation occurs). In the present paper the electronic minimization, which generates the occu-
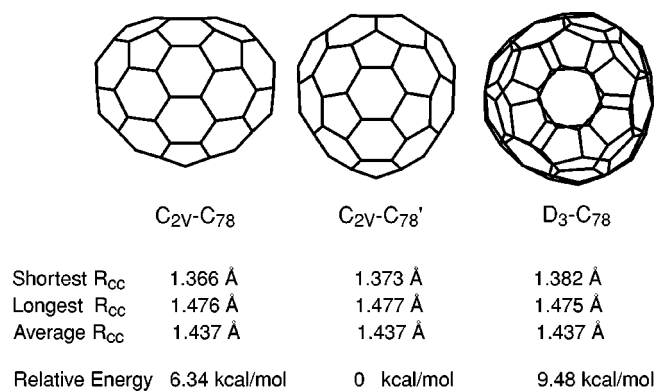
	C_{2V}-C_{78}	C_{2V}-C_{78}'	D_3-C_{78}
Shortest R_{CC}	1.366 Å	1.373 Å	1.382 Å
Longest R_{CC}	1.476 Å	1.477 Å	1.475 Å
Average R_{CC}	1.437 Å	1.437 Å	1.437 Å
Relative Energy	6.34 kcal/mol	0 kcal/mol	9.48 kcal/mol

FIG. 1. The two C_{2v} isomers of C_{78} that are studied in this work. Statistics of bond lengths for the optimized fullerene structures are also shown.

pied electron density, is obtained by using the iglo-iii basis set of Kutzelnigg *et al.*[21] for the excited carbon, and four-electron effective core potentials[22] for the other atoms. The intensities of the x-ray absorption spectral lines are derived from the computed dipole transition moments for excitations from the core (C1s). The use of the full core-hole potential gives excellent transition moments for evaluation of XAS intensities as well as good relative energy positions of the intensities for similar systems.[14] In order to obtain also absolute energy positions of the peaks, the spectra are calibrated so that the first spectral feature, corresponding to the transition to the lowest unoccupied orbital (LUMO) coincides with the calculated excitation energy of the C1s to the LUMO. This is obtained by using a ΔKS (Kohn-Sham) scheme involving the calculation of the energy difference between the ground state and the fully optimized core-excited state. Note that this calibration is done without any comparison with experiment, which makes it a powerful predictive tool. Ionization potentials (IP's) are also computed using the ΔKS scheme, that is, as the energy difference between the ground state and the fully optimized core-ionized state. The relativistic correction has been taken into account. The XA spectra are brought into a final form using a Gaussian function with full width at half maximum (FWHM) of 0.5 eV in order to convolute the oscillator strengths before the IP, while in the continuum, above the IP, the spectra are obtained by means of a Stieltjes imaging approach.[23,24] XPS spectra are simply generated from the computed IP's of the different symmetry independent carbon atoms through a convolution with a Gaussian function of FWHM=0.15 eV.

III. RESULTS AND DISCUSSIONS

A. Structures

The structures of the three isomers, labeled C_{2v}-C_{78} (the isomer with 21 independent carbon atoms) C_{2v}'-C_{78} (the isomer with 22 independent carbon atoms), and D_3-C_{78} (the isomer with 13 independent carbon atoms) are shown in Fig. 1, where some statistics of the computed bond lengths are reported as well. The calculations are in agreement with previous investigations,[25] where the C_{2v}-C_{78} isomer was found
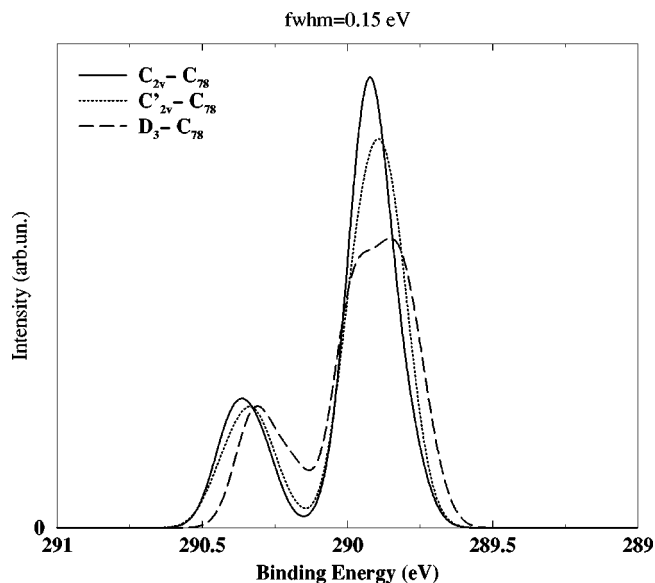
C_{78} calculated XPS spectra

FIG. 2. 1s ionization potentials (IP) for the three C_{78} isomers; the solid line corresponds to the 21 different IP of C_{2v}-C_{78}, the dotted line to the 22 different IP of C_{2v}'-C_{78} and the long dashed line to the 13 different IP of D_3-C_{78}.

to be less stable than C_{2v}'-C_{78}, but more stable than the D_3-C_{78} isomer. In the present paper we have found that the energy of the C_{2v}-C_{78} isomer is about 6.34 kcal/mol higher than the C_{2v}'-C_{78} isomer, and 3.14 kcal/mol lower than the D_3-C_{78} isomer.

It is widely used to group the carbon atoms of fullerenes according to the local environment. Three types of carbon sites are commonly distinguished:[3,26] (1) the pyracylene site, where the carbon atom lying in a pentagon is joined through an exo bond to another pentagon; (2) the corannulene site where the carbon atom lying in pentagon ring is joined through an exo bond to a hexagon; (3) the pyrene site where the carbon is part of three hexagons. By considering the structure of a large fullerene as generated from C_{60}, it is to be noted that the pyracylene and corannulene sites are originated from C_{60} itself, while the pyrene site is introduced by the extra carbons that have been added to the C_{60} molecule to form the larger fullerene. The different combinations of the pyracylene and corannulene sites result in the different isomers. For instance, there are 34 pyracylene sites and 26 corannulene sites for C_{2v}-C_{78}, and 26 pyracylene sites and 34 corannulene sites for C_{2v}'-C_{78}. The 60 nonpyrene atoms are instead divided in 36 pyracilene and 24 corannulene sites for D_3-C_{78} (Fig. 1).

B. Photoelectron Spectra

There are two distinct features in the XPS spectra of all three C_{78} isomers, as demonstrated by the calculated photoelectron spectra presented in Fig. 2. It is noticed that the carbon atoms that give rise to the peak at lower energies belong to the pyracylene and corannulene sites, while the peak at higher energy is associated with carbon atoms in the pyrene sites. This also explains the computed approximate

3:1 intensity (area) ratio for these two features. It indicates that within the higher fullerenes, the local environment changes have relatively small impact on the C1s ionization potentials of those 60 carbons originated from the C_{60}, while the major chemical shifting is caused by the extra carbons that are added on. Such a feature might thus become useful to roughly distinguish different fullerenes.

Ionization energies of the C1s electron do not allow visible discrimination of the two isomers with the same symmetry, as shown in Fig. 2, since C_{2v}-C_{78} and $C_{2v'}$-C_{78} generate almost identical XPS signals with two peaks arising at 289.9 eV and 290.3 eV. The isomer with D_3 symmetry produces a slightly different XPS spectrum, where the main spectral features appear broader than the corresponding features generated by the C_{2v} isomers. Consequently XPS may in principle be employed as a tool to identify isomers with different symmetry.

C. X-ray Absorption Spectra

Of more interest to us are the C1s XA spectra where an electron is excited to the unoccupied molecular orbitals. The so-formed x-ray absorption spectra at the carbon K edge show specific transitions for each of the two isomers. In Fig. 3 the theoretical XA spectra of two C_{2v} isomers are compared with the corresponding experimental measurements.[11] The total spectra are obtained by computing the XA spectra for the symmetry-independent atoms (21 carbons in one case and 22 in the other case) and summing up the different contributions scaled with the relative abundance of every type of carbon atom. The specific peaks that distinguish one isomer from another are correctly predicted by the calculations, which are thus accurate enough in order to mimic the variation of local environments of the independent carbons of the two isomers.

The analysis of the spectra of the two C_{2v} isomers is hampered by the high delocalization of the valence orbitals and the rather low symmetry of C_{78}, as well as the elevated number of symmetry-independent atoms. In the discrete spectrum of C_{60}, for which there is only one symmetry-independent carbon due to the icosahedral symmetry, only four electronic levels occur. Based on a ground-state picture these levels can be classified as t_{1u}, t_{1g}, t_{2u}, and h_g in increasing energy order.[14] Such a degeneracy is removed in the C_{2v} structure of C_{78}, allowing then a high number of different transitions.

A comparison between the spectrum of C_{2v}-C_{78} and the one of $C_{2v'}$-C_{78} suggests that, despite of the variety of possible transitions, the total spectra of both the isomers can still be reduced to the presence of three significant features. These features are pinpointed in Fig. 3 and in Table I we report the corresponding energies. The first and the third peaks (the peaks are numbered according to the order of appearance) arise distinctly in both the spectra, while the second feature, which is clear in the spectrum of $C_{2v'}$-C_{78} is not readily perceived for C_{2v}-C_{78}. The importance of that feature will be explained below. The first and the third peaks are separated by 1.8 eV for both isomers and the energies of these two transitions appear not to be much isomer depen-

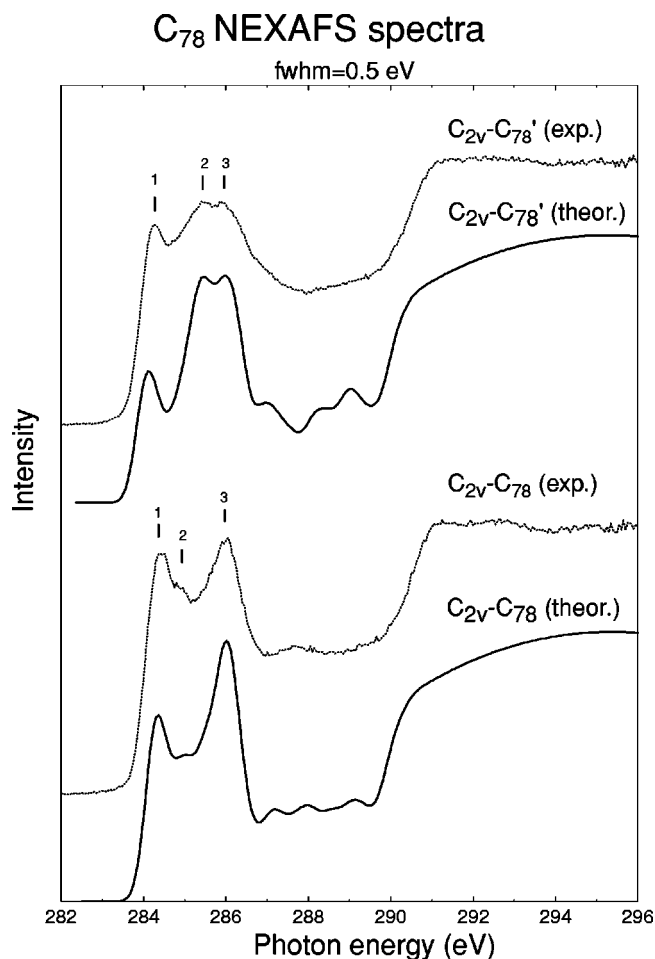FIG. 3. Calculated NEXAFS spectra (thick solid line) for the two C_{2v} C_{78} isomers. A Δ KS scheme is applied to compute the excitation energy to the lowest unoccupied orbital (LUMO). The experimental data (thin solid line) are taken from Ref. 11.

TABLE I. Energies for the three significant features in the near-edge x-ray-absorption fine structure (NEXAFS) spectra of the two C_{78} isomers. Data for C_{70} are taken from Ref. 14.

System	Feature 1 (eV)	Feature 2 (eV)	Feature 3 (eV)
C_{2v}-C_{78}	284.3	285.1	286.1
Pyracylene	284.3		286.0
Corannulene	284.4		286.1
Pyrene		285.1	286.1
$C_{2v'}$-C_{78}	284.2	285.5	286.0
Pyracylene	284.2		285.9
Corannulene	284.1	285.3	286.2
Pyrene		285.5	
C_{70}	284.6	285.4	286.4
Pyracylene	284.6	285.6	286.5
Corannulene	284.5	285.3	286.4
Pyrene		285.3	286.5

C_{2v}-C_{78} calculated NEXAFS spectra
fwhm=0.5 eV

FIG. 4. Calculated NEXAFS spectrum with the individual components for the three different types of carbon atoms in C_{2v}-C_{78}. These components are obtained by summing the individual spectra of the independent carbon atoms according to the pyracylene, corannulene, pyrene classification and scaling by their relative abundance.
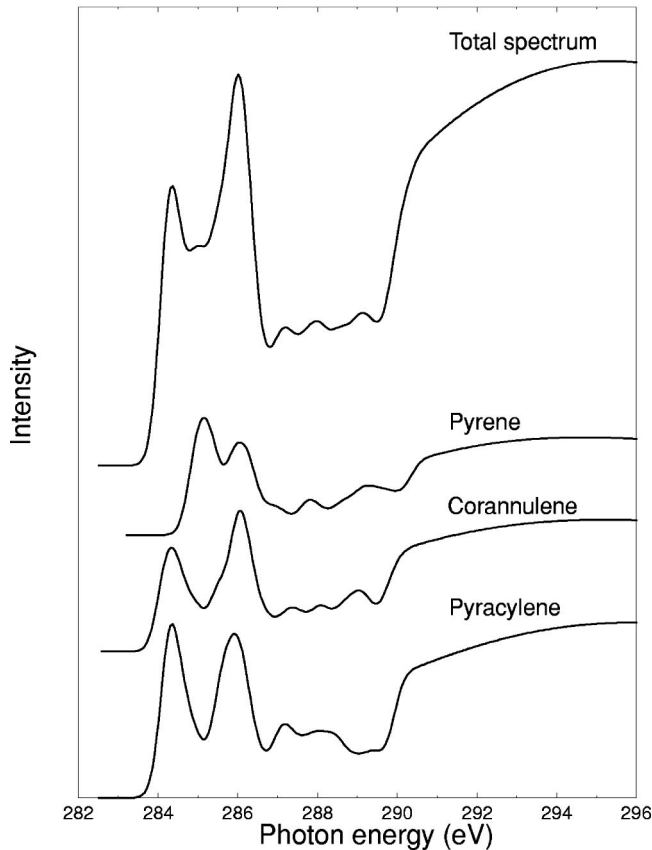
C_{2v}-C_{78}' calculated NEXAFS spectra
fwhm=0.5 eV

FIG. 5. Calculated NEXAFS spectrum with the individual components for the three different types of carbon atoms in $C_{2v'}$-C_{78}. These components are obtained by summing the individual spectra of the independent carbon atoms according to the classification in pyracylene, corannulene, pyrene sites and scaling by their relative abundance.

dent, being almost similar in the two spectra. In contrast, the relative position of the second peak depends on the isomeric form of C_{78}; this feature is lower in energy and closer to the first peak in C_{2v}-C_{78} and higher in energy, closer to the second peak in $C_{2v'}$-C_{78}. For the C_{2v}-C_{78} fullerene, including 21 independent carbon atoms the energy separation between the first and the second peak is 0.8 eV, which increases to 1.3 eV for the other isomer. The peculiar behavior of this feature produces the main differences in the spectra of the two isomers and constitutes the isomer dependence of the XA spectra. Its origin can be understood from the decomposition of the total spectra of the isomers according to the classification of the carbon atoms given above, as shown in Figs. 4 and 5.

The comparison of the decomposed spectra with the corresponding total ones shows that, for both the isomers, the first and the third peaks are significantly contained in the spectra originated by the pyracylene and the corannulene sites. The second peak instead stems primarily from excitations of the pyrene component, that is, by the carbon atoms that only connects to hexagon rings. Mulliken population
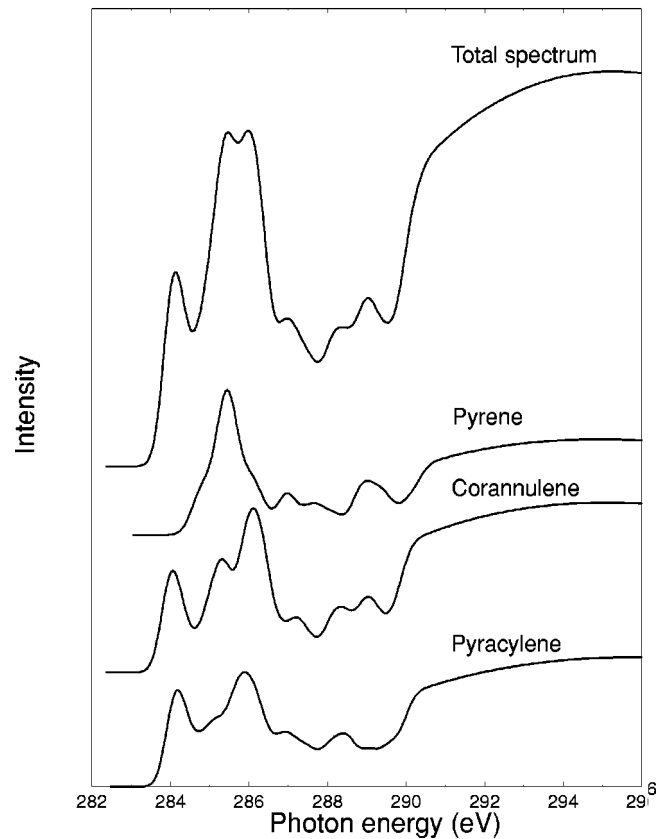
analysis of the orbitals confirms that such a peak is associated with a molecular orbital originated from carbons lying only on hexagons. The second feature can thus reasonably be considered as the fingerprint of the specific isomer, allowing a distinction of the two fullerenes through the XA spectra. The pyrenelike carbon contribution in the spectra was discussed also in connection with the previous calculations performed on C_{70},[14] where a feature was found between the first and the third peaks, similar to the corresponding C_{78} case (see Table I), which can again be considered as a fingerprint of the fullerene. The second feature is indeed connected to the presence of carbons sharing three hexagons, and it determines the particular shape of the XA spectrum for C_{70}.

Higher in energy, at around 287.8 eV, a less prominent feature arises in the experimental C_{2v}-C_{78} spectrum, which is not present in the $C_{2v'}$-C_{78} spectrum. At first sight calculations do not perform well for this peculiar feature since it is not accurately reproduced in the theoretical spectrum. However, further below we will discuss why the experimental spectrum of C_{2v}-C_{78} does not allow a one-to-one comparison in the specific case of this feature. This fingerprint of the isomers is less pronounced than the intensity changes of the

second peak mentioned above, so the conclusions that can be drawn from this higher-energy feature are more vague.

While calculations can accurately predict the position of the different peaks, and particularly the shift of the characteristic second peak in the two isomers, the experimental intensities are not exactly reproduced, which was also observed in the previous theoretical investigation of C_{70};[14] for example, the intensity ratio between the third and the first feature is smaller than the experimental one. This behavior could be due to some vibronic coupling effects that are expected to be stronger in the region of the third feature due to the relatively high density of states present in this region. Consequently a broadening of this peak is expected if these effects are included, resulting in a decreased height of the peak itself. Further, relaxation effects could also contribute to alter the theoretical intensity ratio.[27] It is worth mentioning that after the full core-hole calculation, which gives the dipole moments and the relative energies of the different transitions, the whole spectra are shifted in order to include relaxation effects within a Δ KS scheme. The computational cost of these calculations and the large number of transitions (i.e., the large number of independent carbons) allow us to estimate the relaxation effects only for the first transition. We have, therefore, approximated the effects of final-state relaxations by shifting all the calculated spectra according to the relaxation effects relative to the first transition. This procedure is expected to work well for π^*-like features in the spectra, while for Rydberg-type orbitals smaller relaxation effects are expected. Slightly different relaxation for the orbitals at higher energies could produce a broadening of the peaks and a consequent lower peak height.

Recently we were informed that the experimental spectrum of C_{2v}-C_{78} shown in Fig. 3 was not generated from the pure C_{2v}-C_{78} isomer, and a possible D_3-C_{78} contamination was discovered.[28] It was revealed by the new experimental studies that the small feature around 288 eV in the old spectrum of C_{2v}-C_{78} is actually associated with the D_3-C_{78} isomer.[28] Remarkably, the calculated XA spectrum of D_3-C_{78} isomer does show a distinct feature at 287.5 eV, which is nicely illustrated in Fig. 6. This also explains why some difficulties were encountered in reproducing theoretically the feature arising at about the same energy in the C_{2v}-C_{78} spectrum. Our calculation indicates that the contamination of D_3-C_{78} isomer can make the second spectral peak of C_{2v}-C_{78} isomer broader, which is indeed what has been observed experimentally. Furthermore, the calculated spectrum of D_3-C_{78} isomer is found to be in excellent agreement with the corresponding experimental result.[28] It can thus be concluded from Fig. 6 that the identification of the isomers can be easily realized by using the XA spectra.

We find that these studies are encouraging in the sense that it is possible to accurately calculate XA intensities for such large systems as C_{78}. However, we also wish to mention the difficulties of generating fullerene XA spectra based on a building-block principle. By inspection of Figs. 4 and 5, we find that it is impossible to generate the spectrum of one of the isomers by using the calculated spectral components
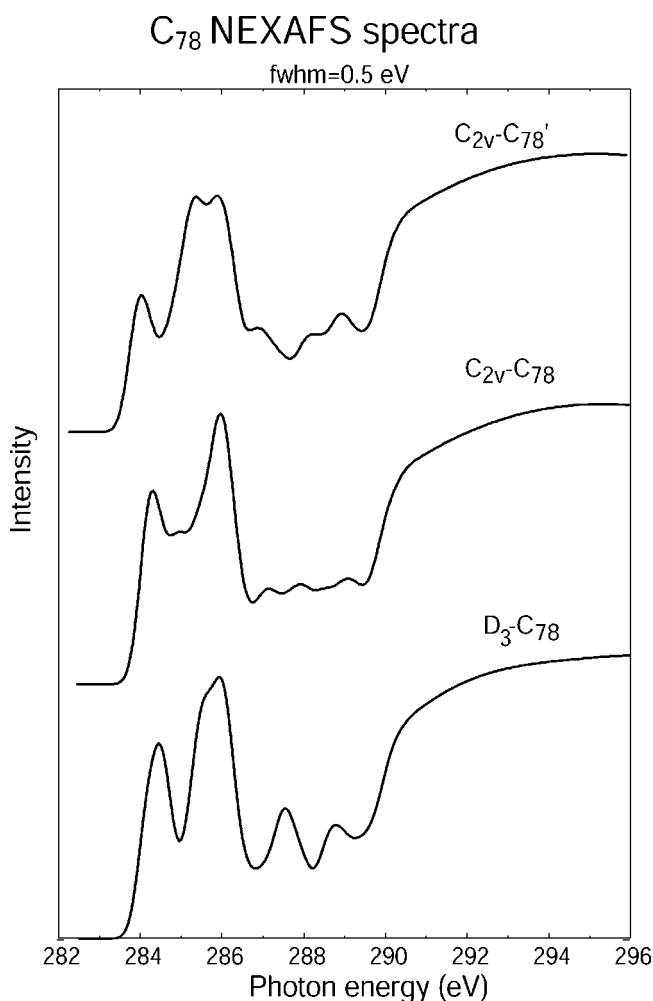

FIG. 6. Calculated NEXAFS spectra of three isomers.

of the other isomer and vice versa. Especially, the energy position of the spectral pyrene component seems to vary with the global arrangement of carbon atoms rather than just the three nearest neighbors.

IV. CONCLUSIONS

Theoretical XA spectra for three isomers of C_{78} are in remarkable agreement with the corresponding experimental measurements. The calculations performed at the DFT level of theory allow us to highlight the origin of the main significant differences between the two spectra. Particularly, the carbon atoms present at the fusion of three hexagon rings (pyrene sites) generate a signal that is characteristic of the isomer, which is responsible for the specific shape of the spectrum.

*Email address: luo@theochem.kth.se

[1] H.W. Kroto, J.R. Heath, S.C. O'Brien, R.F. Curl, and R.E. Smalley, Nature (London) **318**, 162 (1985).

[2] R. Ettl, I. Chao, F. Diederich, and R.L. Whetten, Nature (London) **353**, 149 (1991).

[3] F. Diederich and R.L. Whetten, Acc. Chem. Res. **25**, 119 (1992).

[4] K. Kikuchi, N. Nakahara, T. Wakabayashi, S. Suzuki, H. Shiromaru, Y. Miyake, K. Saito, L. Ikemoto, M. Kainosho, and Y. Achiba, Nature (London) **357**, 142 (1992).

[5] R. Taylor, G.J. Langley, A.G. Avent, T.J.S. Dennis, H.W. Kroto, and D.R.M. Walton, J. Chem. Soc., Perkin Trans. **2**, 1029 (1993).

[6] F.H. Hennrich, R.H. Michel, A. Fischer, S. Richard-Schneider, S. Gilb, M.M. Kappes, D. Fuchs, M. Bürk, K. Kobayashi, and S. Nagase, Angew. Chem. Int. Ed. Engl. **35**, 1732 (1996).

[7] T.J.S. Dennis, T. Kai, T. Tomiyama, and H. Shinoara, Chem. Commun. (Cambridge) **1999**, 1023 (1999).

[8] M. Benz, M. Fanti, P.W. Fowler, D. Fuchs, M.M. Kappes, C. Lehner, R.H. Michel, G. Orlandi, and F. Zerbetto, J. Phys. Chem. **100**, 13 399 (1996).

[9] Y. Achiba, K. Kikuchi, M. Muccini, G. Orlandi, G. Ruani, C. Taliani, R. Zamboni, and F. Zerbetto, J. Phys. Chem. **98**, 7933 (1994).

[10] P.W. Fowler and D.E. Manolopoulos, *An Atlas of Fullerenes* (Oxford University Press, New York, 1995).

[11] M. Knupfer, O. Knauff, M.S. Golden, J. Fink, M. Bürk, D. Fuchs, S. Schuppler, R.H. Michel, and M.M. Kappes, Chem. Phys. Lett. **258**, 513 (1996).

[12] L. Triguero, L.G.M. Pettersson, and H. Ågren, Phys. Rev. B **58**, 8097 (1999).

[13] M. Nyberg, J. Hasselström, O. Karis, N. Wassdahl, M. Weinelt, A. Nilsson, and L.G.M. Pettersson, J. Chem. Phys. **112**, 5420 (2000).

[14] M. Nyberg, Y. Luo, L. Triguero, L.G.M. Pettersson, and H. Ågren, Phys. Rev. B **60**, 7956 (1999).

[15] S. Carniato, Y. Luo, and H. Ågren, Phys. Rev. B **63**, 085105 (2001).

[16] M.J. Frisch, G.W. Trucks, H.B. Schlegel, G.E. Scuseria, M.A. Robb, J.R. Cheeseman, V.G. Zakrzewski, J.A. Montgomery, Jr., R.E. Stratmann, J.C. Burant, S. Dapprich, J.M. Millan, A.D. Daniels, K.N. Kudin, M.C. Strain, O. Farkas, J. Tomasi, V. Barone, M. Cossi, R. Cammi, B. Mennucci, C. Pomelli, C. Adamo, S. Clifford, J. Ochterski, G.A. Petersson, P.Y. Ayala, Q. Cui, K. Morokuma, D.K. Malick, A.D. Rabuck, K. Raghavachari, J.B. Foresman, J. Cioslowski, J.V. Ortiz, B.B. Stefanov, G. Liu, A. Liashenko, P. Piskorz, I. Komaromi, R. Gomperts, R. L. Martin, D.J. Fox, T. Keith, M.A. Al-Laham, C.Y. Peng, A. Nanayakkara, C. Gonzalez, M. Challacombe, P.M.W. Gill, B. Johnson, W. Chen, M.W. Wong, J.L. Andres, M. Head-Gordon, E.S. Replogle, and J.A. Pople, GAUSSIAN 98 (Gaussian Inc., Pittsburgh, PA, 1998).

[17] M.E. Casida, C. Daul, A. Goursot, A. Koester, L.G.M. Pettersson, E. Proynov, A. St-Amant, and D.R. Salahub, DEMON-KS version 4.0 (deMon Software, Montréal, 1997).

[18] J. Perdew and Y. Wang, Phys. Rev. B **33**, 8800 (1986).

[19] J. Perdew, Phys. Rev. B **34**, 7406 (1986).

[20] H. Ågren, V. Carravetta, O. Vahtras, and L.G.M. Pettersson, Chem. Phys. Lett. **222**, 75 (1994).

[21] W. Kutzelnigg, U. Fleisher, and M. Shindler, *NMR-Basic Principles and Progress* (Springer-Verlag, Heidelberg, 1990).

[22] L.G.M. Pettersson (unpublished).

[23] P.W. Langhoff, *Electron-Molecule and Photon-Molecule Collisions* (Plenum, New York, 1979).

[24] P.W. Langhoff, *Theory and Application of Moment Methods on Many-Fermion Systems* (Plenum, New York, 1980).

[25] G. Sun and M. Kertesz, J. Phys. Chem. A **104**, 7398 (2000).

[26] T. Heine, G. Seifert, P.W. Fowler, and F. Zerbetto, J. Phys. Chem. A **103**, 8738 (1999).

[27] C. Kolczewski, R. Püttner, O. Plashkevych, H. Agren, L.G.M. Pettersson, M. Martins, G. Snell, A.S. Schlachter, M. Sant'anna, G. Kaindl, and V. Staemmler, J. Chem. Phys. **115**, 6426 (2001).

[28] R. Friedlein (private communication).